Inorg. Chem. **2005**, *44*, 7523–7529

Magnetic Properties of Isostructural $BaCoP_2O_7$, $BaNiP_2O_7$, and $BaCuP_2O_7$ Studied with dc and ac Magnetization and Specific Heat

Alexei A. Belik,*[†,‡,§] Masaki Azuma,[†,‡] and Mikio Takano[†]

International Center for Young Scientists (ICYS), National Institute for Materials Science, Namiki 1-1, Tsukuba, Ibaraki, 305-0044, Japan, Institute for Chemical Research, Kyoto University, Uji, Kyoto-fu 611-0011, Japan, and PRESTO, Japan Science and Technology Corporation (JST), Kawaguchi, Saitama 332-0012, Japan

Received June 10, 2005

Magnetic properties of three isostructural compounds $BaMP_2O_7$ (M = Co, Ni, and Cu) were investigated by dc and ac magnetization and specific heat measurements. $BaCuP_2O_7$ was shown to be an excellent quasi-one-dimensional linear-chain Heisenberg antiferromagnet with an exchange constant (J/k_B) of 103.8 K (Hamiltonian $H = J\sum S_iS_{i+1}$) and a temperature for the long-range magnetic order (T_N) of 0.81 K giving the ratio $k_BT_N/J = 0.78\%$. $BaCoP_2O_7$ and $BaNiP_2O_7$ exhibited long-range antiferromagnetic order at $T_N = 10.4$ and 10.1 K, respectively. $BaCoP_2O_7$ and $BaNiP_2O_7$ showed a large contribution of the short-range correlation above T_N. $BaNiP_2O_7$ remained in the antiferromagnetic state up to 90 kOe at 2 K, whereas $BaCoP_2O_7$ demonstrated two metamagnetic phase transitions at about 52 and 71 kOe at 2 K if the magnetic field was parallel to the easy direction. $BaMP_2O_7$ melted incongruently at 1323 K (M = Co), 1344 K (M = Ni), and 1338 K (M = Cu).

Introduction

Low-dimensional quantum magnets have attracted considerable attention because of their interesting physical properties. Quantum phenomena in a one-dimensional (1D) zigzag chain with the next-nearest-neighbor (NNN) interaction (double-spin chain system) have recently been studied from both theoretical and experimental viewpoints.[1−6] Spin interactions in such a system, shown in Figure 1a, are described by three exchange constants (J_1, J_2, and J_3). Depending on the ratio between J_1, J_2, and J_3, this spin system can have a gapped ground state or can be gapless. In the case of $J_1 = J_2$, it gives the so-called railroad-trestle model.[1−3] For $J_1 = 0$ or $J_2 = 0$, the ordinary two-leg ladder system is obtained.

Three isostructural $BaMP_2O_7$ compounds (M = Co, Ni, and Cu)[7−9] are the candidate model compounds for the S = 3/2, 1, and 1/2 (S is spin) zigzag chain with NNN interactions. They crystallize in space group $P\bar{1}$ with $a = 7.353$ Å, $b = 7.578$ Å, $c = 5.231$ Å, $\alpha = 90.83°$, $\beta = 95.58°$, and $\gamma = 103.00°$ (for $BaCuP_2O_7$).[9] Note that $BaCoP_2O_7$ and $BaNiP_2O_7$ exhibit an incommensurate modulated structure at room temperature.[7,8] M^{2+} ions have square-pyramidal coordination. There are obvious structural dimer units formed by two edge-shared MO_5 polyhedra (Figure 1b). The dimer units are connected with each other through two super-superexchange interactions Cu−O···O−Cu, where the O···O is an edge of a PO_4 group, creating the double-spin chain system. The M−M distance in the dimer unit is 3.32 Å (for $BaCuP_2O_7$). The M−M distances for the interactions transferred through two Cu−O···O−Cu paths are 4.48 and 5.23 Å (for $BaCuP_2O_7$). The arrangement of the double chains is shown in Figure 1c.

$BaZnP_2O_7$ is also isotypic with $BaMP_2O_7$ (M = Co, Ni, and Cu);[10] this makes the estimation of lattice contribution in the specific heat more correct. The magnetic susceptibility

* To whom correspondence should be addressed. International Center for Young Scientists, National Institute for Materials Science, Namiki 1-1, Tsukuba, Ibaraki, 305-0044, Japan. E-mail: Alexei.BELIK@nims.go.jp.
§ ICYS.
† Institute for Chemical Research.
‡ PRESTO.

(1) Maeshima, N.; Okunishi, K. *Phys. Rev. B* **2000**, *62*, 934−939.
(2) Hosokoshi, Y.; Katoh, K.; Inoue, K.; Goto, T. *J. Phys. Soc. Jpn.* **1999**, *68*, 2910−2913.
(3) Hagiwara, M.; Narumi, Y.; Kindo, K.; Maeshima, N.; Okunishi, K.; Sakai, T.; Takahashi, M. *Physica B* **2001**, *294*−*295*, 83−86.
(4) Nakamura, T.; Okamoto, K. *Phys. Rev. B* **1998**, *58*, 2411−2414.
(5) Nakamura, T. *Phys. Rev. B* **1998**, *57*, R3197−R3200.
(6) Haga, N.; Suga, S.-I. *Phys. Rev. B* **2001**, *65*, 014414-1−014414-7.
(7) Riou, D.; Labbe, P.; Goreaud, M. *C. R. Acad. Sci., Ser. II* **1988**, *307*, 903−907.
(8) Riou, D.; Leligny, H.; Pham, C.; Labbe, P.; Raveau, B. *Acta Crystallogr., Sec. B* **1991**, *47*, 608−617.
(9) Moqine, A.; Boukhari, A.; Holt, E. M. *Acta Crystallogr., Sec. C* **1991**, *47*, 2294−2297.

10.1021/ic050938z CCC: $30.25
Published on Web 09/10/2005

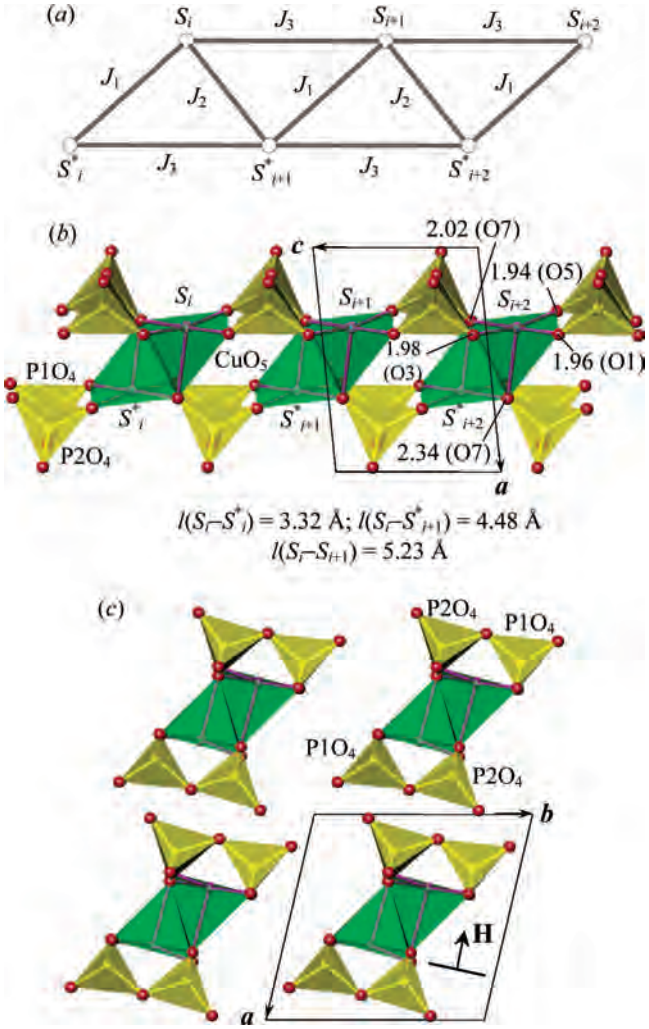

Figure 1. (a) Spin-interaction scheme for the bond-alternating zigzag chain with the next-nearest-neighbor interaction (double-spin chain model). (b) Projection of the structure of $BaCuP_2O_7$ along the *b* direction emphasizing the Cu−Cu chains in the *c* direction. Cu−O distances are given in Å. (c) Projection of the structure of $BaCuP_2O_7$ along the *c* direction. Arrangement of the double Cu chains.

of $BaCuP_2O_7$ was measured by Boukhari et al.[11] at 4.2−300 K; however, no maximum characteristic of low-dimensional magnets was observed, probably because of the large Curie−Weiss contribution from impurity spins coming from a poor-quality sample.

We have recently investigated the magnetic properties of $ACuP_2O_7$ (A = Ca, Sr, Ba, and Pb)[12,13] and $ACuV_2O_7$ (A = Sr and Ba)[14] whose magnetic sublattice can be described, from the structural point of view, by the model shown in Figure 1a. The experimental data for $ACuP_2O_7$ (A = Ca, Sr, Ba, and Pb) agreed with the 1D $S = 1/2$ Heisenberg antiferromagnetic uniform-chain model with almost negligible NNN interactions. In the case of $ACuV_2O_7$ (A = Sr and Ba), the main intrachain interaction was found to be ferromagnetic.[14]

In this work, we have studied properties of $BaMP_2O_7$ (M = Co, Ni, and Cu) by dc and ac magnetization and specific heat measurements. The experimental data agreed well with the assumption of the presence of the 1D uniform linear chains in $BaCuP_2O_7$ ($J_3 = 103.8$ K) with almost negligible J_1 and J_2. $BaCoP_2O_7$ and $BaNiP_2O_7$ exhibited a long-range antiferromagnetic order at $T_N = 10.4$ and 10.1 K, respectively, whereas T_N is 0.81 K in $BaCuP_2O_7$. $BaCoP_2O_7$ and $BaNiP_2O_7$ showed a large contribution from short-range correlations above T_N. $BaNiP_2O_7$ remained in the antiferromagnetic state up to 90 kOe at 2 K, whereas $BaCoP_2O_7$ demonstrated two metamagnetic phase transitions at about 52 and 71 kOe at 2 K. We have also investigated the thermal stability of $BaMP_2O_7$ (M = Co, Ni, and Cu) in air.

Experimental Section

Preparation. The $BaMP_2O_7$ compounds (M = Co, Ni, Cu, and Zn) were prepared from stoichiometric mixtures of $BaCO_3$ (99.99%), Co_3O_4 (99.9%), NiO (99.9%), CuO (99.99%), ZnO (99.9%), and $NH_4H_2PO_4$ (99.8%) by the solid-state method. The mixtures were heated very slowly from room temperature to 770 K in alumina crucibles. Then they were reground, pressed into pellets at 200 kgf/cm^2, and allowed to react at 1173 K for $BaCoP_2O_7$ and $BaCuP_2O_7$, at 1283 K for $BaNiP_2O_7$, and at 1243 K for $BaZnP_2O_7$ on Pt plates for 100 h with four intermediate grindings. X-ray powder diffraction (XRD) data collected with a RIGAKU RINT 2500 diffractometer (2θ range of 8−60°, a step width of 0.02°, and a counting time of 1 s/step) showed that the $BaMP_2O_7$ (M = Co, Cu, and Zn) compounds were monophasic, whereas $BaNiP_2O_7$ contained small amount of an unknown impurity and $Ba_2Ni(PO_4)_2$.

The aligned polycrystalline samples for the detailed magnetic studies were prepared by applying a magnetic field of 90 kOe at 300 K to mixtures of $BaMP_2O_7$ (M = Co and Cu) and epoxy resin (Stycast 1266). $BaCuP_2O_7$ was aligned in a manner where the basal planes of the CuO_5 pyramids were perpendicular to the applied magnetic field (Figure 1c). This kind of alignment resulted in very strong (200), (−310), (−410), and (400) reflections on the XRD patterns. The alignment direction for $BaCoP_2O_7$ was more difficult to determine (see the XRD patterns in the Supporting Information). From the indices of the peaks with increased intensity, we could conclude that the applied magnetic field was approximately perpendicular to the Co−Co bond in the dimer unit.

Magnetic and Specific Heat Measurements. Magnetic susceptibilities, $\chi = M/H$, of $BaMP_2O_7$ (M = Co, Ni, and Cu) were measured on a SQUID magnetometer (Quantum Design, MPMS XL) between 2 and 300 (or 400) K in applied fields of 0.1 and 10 kOe under both zero-field-cooled (ZFC) and field-cooled (FC) conditions. Note that magnitudes of χ for the aligned samples are not exact because we cannot exactly estimate the quantity of the powder contained in the resin. Magnetization measurements were performed between 0 and 90 kOe at 2 and 5 K using a Quantum Design PPMS instrument. Magnetic susceptibilities for $BaCoP_2O_7$ were also measured at 90 kOe under FC conditions from 110 to 2 K using the PPMS. The temperature and field dependence of the ac magnetic susceptibility (in-phase component, $\chi' = M'/H_{ac}$, and out-of-phase component, $\chi'' = M''/H_{ac}$) were measured at frequencies (f) of 10, 10^2, 10^3, 5×10^3, and 10^4 Hz and at applied oscillating magnetic fields (H_{ac}) of 1 and 10 Oe using the PPMS. Specific

(10) Murashova, E. V.; Velikodnyi, Yu. A.; Trunov, V. K. *Russ. J. Inorg. Chem.* **1991**, *36*, 847−850.
(11) Boukhari, A.; Moqine, A.; Flandrois, S. *J. Solid State Chem.* **1990**, *87*, 251−256.
(12) Belik, A. A.; Azuma, M.; Takano, M. *Inorg. Chem.* **2003**, *42*, 8572−8578.
(13) Belik, A. A.; Azuma, M.; Takano, M. *J. Magn. Magn. Mater.* **2004**, *272−276*, 937−938.
(14) Belik, A. A.; Azuma, M.; Matsuo, A.; Kindo, K.; Takano, M. *Inorg. Chem.* **2005**, *44*, 3762−3766.

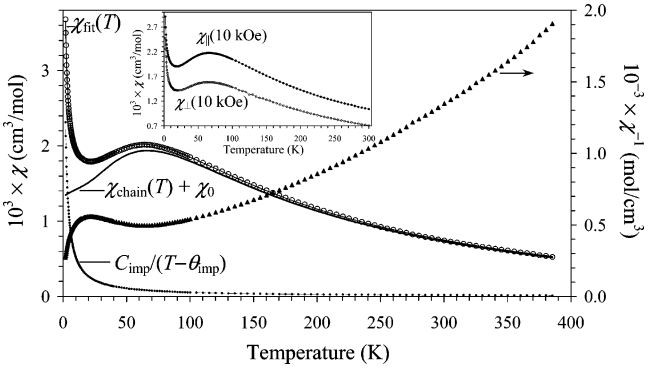

Figure 2. Magnetic susceptibilities, χ and χ^{-1} (ZFC curves; symbols), against temperature, T, for the powder $BaCuP_2O_7$ sample measured at 100 Oe. Solid line represents the fit by eqs 1 and 2, $\chi_{fit}(T)$. Solid lines with small dots are contributions of $\chi_0 + \chi_{chain}(T)$ and $C_{imp}/(T - \theta_{imp})$. Inset presents the $\chi_{||}(T)$ and $\chi_{\perp}(T)$ curves measured at 10 kOe for the aligned $BaCuP_2O_7$ sample.

heat, C_p, for the powder samples was recorded between 0.40 (or 2) and 55 K (on cooling) by a pulse-relaxation method using a commercial calorimeter (PPMS). For $BaCoP_2O_7$, the $C_p(T)$ data were also taken at magnetic fields of 50 and 90 kOe from 55 to 2 K.

Thermal Analysis. The thermal stability of $BaMP_2O_7$ (M = Co, Ni, and Cu) was examined under air with a MacScience TG-DTA 2000 instrument. The samples were placed in Pt crucibles, heated, and then cooled at a rate of 10 K/min. The $BaMP_2O_7$ (M = Co, Ni, and Cu) compounds were shown to be stable up to 1323, 1344, and 1338 K, respectively. The large inconsistency in the heating and cooling behavior suggested that they melt incongruently.

Results and Discussion

Figure 2 presents plots of χ and χ^{-1} (ZFC curves) against temperature, T, for $BaCuP_2O_7$. No noticeable difference was found between the curves measured under the ZFC and FC conditions. The $\chi(T)$ data exhibited a broad maximum at T_M = 66.1 K, characteristic of low-dimensional systems. However, the $\chi(T)$ data did not exhibit the vanishing behavior below T_M characteristic of spin gap compounds, but tended to approach toward finite values typical for gapless quasi-1D systems. The possibility of the dimer model (J_1 is dominant) and two-leg ladder model (J_2 and J_3 are comparable) should therefore be ruled out. The $\chi(T)$ data were fitted very well in the entire temperature range by the equations

$$\chi_{fit}(T) = \chi_0 + C_{imp}/(T - \theta_{imp}) + \chi_{chain}(T) \quad (1)$$

$$\chi_{chain}(T) = \frac{Ng^2\mu_B{}^2}{4k_BT} \frac{1 + \sum_{n=1}^{5} N_n/t^n}{1 + \sum_{n=1}^{6} D_n/t^n} \quad (2)$$

where $\chi_{chain}(T)$ is the spin susceptibility curve of the uniform $S = 1/2$ Heisenberg antiferromagnetic chain parametrized by Johnston et al. (eq 50 in ref 15), $t = k_BT/J$, N is Avogadro's number, g is the spectroscopic splitting factor (g factor), μ_B is the Bohr magneton, k_B is Boltzmann's constant, C_{imp} is an impurity Curie constant, θ_{imp} is an impurity Weiss constant, χ_0 is the temperature independent term, and J is the exchange constant with the Hamiltonian formulated as $H = J\sum S_iS_{i+1}$: $N_1 = -0.053837836$, $N_2 = 0.097401365$, $N_3 = 0.014467437$, $N_4 = 0.0013925193$, $N_5 = 0.00011393434$, $D_1 = 0.44616216$, $D_2 = 0.32048245$, $D_3 = 0.13304199$, $D_4 = 0.037184126$, $D_5 = 0.0028136088$, and $D_6 = 0.00026467628$. The fitted parameters and measurements of the quality of fits (σ_{rms} and R) are given in Table 1. The magnetic susceptibilities calculated with eqs 1 and 2, $\chi_{fit}(T)$, are plotted in Figure 2.

Table 1. Fitted Parameters for $\chi(T)$, $C_p(T)$, and $\chi^{-1}(T)$ of $BaCuP_2O_7$, $BaCoP_2O_7$, and $BaNiP_2O_7$

eq	quantity	$BaCuP_2O_7$	$BaCoP_2O_7$	$BaNiP_2O_7$
1 and 2	temp range (K)	2−400		
	χ_0 (cm^3/mol)	$-4.17(4) \times 10^{-4}$		
	C_{imp} (cm^{3}K/mol)	$5.43(2) \times 10^{-3}$		
	θ_{imp} (K)	−0.352(12)		
	g	2.105(8)		
	J/k_B (K)[a]	103.8(2)		
	σ_{rms} (%)[b]	0.447		
	R[c]	1.67×10^{-5}		
3	temp range (K)	2−10		
	γ (J K^{-2} mol^{-1})	$5.293(6) \times 10^{-2}$		
	β_1 (J K^{-4} mol^{-1})	$3.61(3) \times 10^{-4}$		
	β_2 (J K^{-6} mol^{-1})	$1.36(3) \times 10^{-6}$		
6	temp range (K)		100−400	50−300
	C (cm^3 K mol^{-1})		2.917(3)	1.4636(10)
	θ (K)		−18.5(2)	−18.06(14)

[a] Hamiltonian $H = J\sum S_iS_{i+1}$. [b] $\sigma_{rms}{}^2 = 1/N_p \sum_{i=1}^{N_p}[(\chi(T_i) - \chi_{fit}(T_i)/\chi(T_i)]^2$, where N_p is the number of data points. [c] $R = \sum_{i=1}^{N_p}(\chi(T_i) - \chi_{fit}(T_i))^2/\sum_{i=1}^{N_p}(\chi(T_i))^2$.

Note that the classical Bonner−Fisher curve[16] (parametrized by Estes et al.)[17] was not applied because it is known that at $k_BT/J < 0.25$, the Bonner−Fisher curve deviates from the recent calculations of spin susceptibility for the uniform $S = 1/2$ chain.[15] In $BaCuP_2O_7$, the temperature range of 2−400 K corresponds to $0.019 < k_BT/J < 3.86$. Note also that the $\chi^{-1}(T)$ curve (Figure 2) deviates from the linear Curie−Weiss behavior in the whole temperature range because of the influence of short-range correlations even at high temperatures.

The $\chi(T)$ data for the aligned $BaCuP_2O_7$ are given on the inset of Figure 2. The $\chi_{||}$ values (i.e., with the magnetic field perpendicular to the basal planes of the CuO_5 pyramids) are larger than the $\chi_{\perp}$ values. This difference can be attributed to g anisotropy. Similar behavior was observed in other 1D systems (e.g., Sr_2CuO_3).[18,19]

Specific heat data were taken at zero field to investigate magnetism of $BaCuP_2O_7$ in more detail. Figure 3 shows the total specific heat divided by temperature, C_p/T, plotted against T. The sharp peak (λ-type anomaly on the $C_p(T)$ curve) was observed at 0.81 K indicating the presence of a long-range magnetic order at this temperature.

Because the present compounds are insulators, specific heat data consist of the magnetic and lattice components.

(15) Johnston, D. C.; Kremer, R. K.; Troyer, M.; Wang, X.; Klümper, A.; Bud'ko, S. L.; Panchula, A. F.; Canfield, P. C. *Phys. Rev. B* **2000**, *61*, 9558−9606.

(16) Bonner, J. C.; Fisher, M. E. *Phys. Rev. A* **1964**, *135*, 640−658.

(17) Estes, W. E.; Gavel, D. P.; Hatfield, W. E.; Hodgson, D. J. *Inorg. Chem.* **1978**, *17*, 1415−1421.

(18) Motoyama, N.; Eisaka, H.; Uchida, S. *Phys. Rev. Lett.* **1996**, *76*, 3212−3215.

(19) Carlin, R. L. *Magnetochemistry*, Springer-Verlag: Berlin, 1986; p 327.

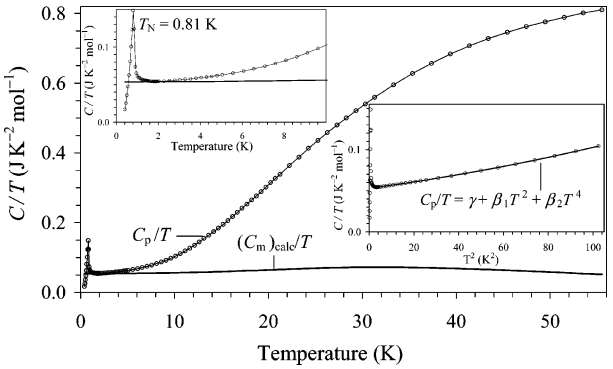

Figure 3. Total specific heat divided by temperature, C_p/T, plotted against T for $BaCuP_2O_7$. Thin solid line between experimental points is drawn for the eye. Thick solid line is the calculated magnetic specific heat divided by temperature, $(C_m/T)_{calcd}$. The left inset shows the enlarged fragment of this figure. The right inset gives the C_p/T vs T^2 curve (symbols) with the fit to eq 3 (solid line).

At low temperatures, the magnetic specific heat divided by temperature, C_m/T, for the uniform $S = 1/2$ Heisenberg antiferromagnetic chain is known to be constant and equal to $(2/3)Nk_B^2/J$.[15] The initial deviation from this constant value is positive and approximately quadratic in T.[15] The lattice contribution can be expressed as $C_l = \beta_1 T^3 + \beta_2 T^5$. Therefore, the experimental C_p/T versus T^2 data can be fitted by the equation

$$C_p/T = \gamma + \beta_1 T^2 + \beta_2 T^4 \qquad (3)$$

where $\gamma = C_m/T$.

We fitted the C_p/T versus T^2 data by eq 3 between 2 and 10 K. The fitted parameters are presented in Table 1. The γ value corresponds to J/k_B of 104.73(11) K, in excellent agreement with the J/k_B value obtained from the magnetic susceptibility data. The value of β_1 gives a Debye temperature, $\Theta_D = (234Nk_B/\beta_1)^{1/3}$, of 175 K for $BaCuP_2O_7$.

The calculated C_m/T curves, $(C_m/T)_{calcd}$, for $BaCuP_2O_7$ are plotted in Figure 3. For our calculations, we used eq 54 from ref 15 (i.e., 1D uniform chain model) and the J/k_B parameter determined from the $\chi(T)$ data

$$C_m(T) = \frac{3Nk_B}{16t^2}\frac{1+\sum_{n=1}^{6}N_n/t^n}{1+\sum_{n=1}^{9}D_n/t^n} - a_1 t \sin\left(\frac{2\pi}{a_2+a_3 t}\right)e^{-a_4 t} - a_5 t e^{-a_6 t} \qquad (4)$$

where $t = k_BT/J$ and the numerical values of the coefficients (N_1-N_6, D_1-D_9, and a_1-a_6) for C_m can be found in ref 15. The $(C_m/T)_{calcd}$ values were very close to the experimental C_p/T values near 2 K, where the lattice contribution and the contribution from the λ-type anomaly are negligible.

Experimental data evidence that magnetic properties of $BaCuP_2O_7$ can be described by the 1D $S = 1/2$ uniform linear-chain model. This fact can be understood using the geometrical parameters of the Cu−O−Cu and Cu−O···O−Cu connections. In the structural dimer unit (J_1), the connection between the Cu atoms includes the long apical Cu−O7 distance (2.34 Å) with the Cu−O7−Cu angle of 99.2°, while the Cu spins occupy $d_{x^2-y^2}$ orbitals lying on the basal planes of the CuO_5 pyramid. (This fact is confirmed by the alignment direction of $BaCuP_2O_7$.) The apical Cu−O7 bonds are also included in J_2. The basal planes of the CuO_5 pyramid lie in different planes for J_1 and J_2, whereas they lie on almost one plane for J_3.[12,20] Therefore, the overlap between the copper $d_{x^2-y^2}$ magnetic orbitals should be almost zero in the case of J_1 and J_2. Thus, in $BaCuP_2O_7$, J_3 ($J_3/k_B = J/k_B = 103.8$ K) is the main exchange constant, and J_1 and J_2 appear to be negligible. The double-spin chain system (Figure 1a) can be considered as two almost isolated 1D linear chains. The recent investigation of exchange interactions in $BaCuP_2O_7$, on the basis of the spin-dimer analysis, confirmed that the main exchange constant is between Cu atoms mediated by two Cu−O···O−Cu paths corresponding to J_3.[21]

The ratio between T_N and J/k_B (k_BT_N/J) is 0.78%. $BaCuP_2O_7$ is therefore an excellent physical realization of the $S = 1/2$ linear-chain Heisenberg antiferromagnet, together with $Sr_2Cu(PO_4)_2$ ($k_BT_N/J = 0.06\%$, $T_N = 85$ mK),[22,23] $Ba_2Cu(PO_4)_2$ ($k_BT_N/J < 0.34\%$),[22] Sr_2CuO_3 ($k_BT_N/J \approx 0.25\%$),[18] γ-LiV_2O_5 ($k_BT_N/J < 0.16\%$),[24] and copper benzoate $Cu(C_6H_5COO)_2 \cdot 3H_2O$ ($k_BT_N/J = 0.0047\%$, $T_N = 0.8$ mK).[25,26] The value of the interchain interaction, $J_\perp/k_B$, in the $S = 1/2$ 1D chain can be estimated using the equation[27]

$$J_\perp/k_B = \frac{T_N}{1.28\sqrt{\ln(5.8J/(k_BT_N))}} \qquad (5)$$

This formula gives $J_\perp/k_B = 0.246$ K. Interchain interactions are ~420 times smaller than J_3 in $BaCuP_2O_7$. ^{31}P NMR studies of $BaCuP_2O_7$ gave similar J/k_B and T_N values.[28]

Figures 4−6 show the $\chi(T)$ and $\chi^{-1}(T)$ curves for $BaCoP_2O_7$ and $BaNiP_2O_7$. There was no difference between the ZFC and FC curves except for the lowest-temperature region, where the upturn in the χ values is caused by the paramagnetic impurities or defects. Between 100 and 400 K for $BaCoP_2O_7$ and 50 and 300 K for $BaNiP_2O_7$, the $\chi^{-1}(T)$ data for the powder samples could be fitted by the simple Curie−Weiss equation

$$\chi(T) = \frac{C}{T-\theta} \qquad (6)$$

where C is the Curie constant and θ is the Weiss constant. The parameters fitted to eq 6 are given in Table 1. $BaCoP_2O_7$

(20) Koo, H.-J.; Whangbo, M.-H.; VerNooy, P. D.; Torardi, C. C.; Marshall, W. J. *Inorg. Chem.* **2002**, *41*, 4664−4672.
(21) Koo, H.-J.; Dai, D.; Whangbo, M.-H. *Inorg. Chem.* **2005**, *44*, 4359−4365.
(22) Belik, A. A.; Azuma, M.; Takano, M. *J. Solid State Chem.* **2004**, *177*, 883−888.
(23) Belik, A. A.; Uji, S.; Terashima, T.; Takayama-Muromachi, E. *J. Solid State Chem.* In press.
(24) Ueda, Y. *Chem. Mater.* **1998**, *10*, 2653−2664.
(25) Asano, T.; Nojiri, H.; Higemoto, W.; Koda, A.; Kadono, R.; Ajiro, Y. *J. Phys. Soc. Jpn.* **2002**, *71*, 594−598.
(26) Karaki, Y.; Masutomi, R.; Kubota, M.; Ishimoto, H.; Asano, T.; Ajiro, Y. *Physica B* **2003**, *329−333*, 1002−1003.
(27) Schulz, H. J. *Phys. Rev. Lett.* **1996**, *77*, 2790−2793.
(28) Nath, R.; Mahajan, A. V.; Buttgen, N.; Kegler, C.; Loidl, A.; Bobroff, J. *Phys. Rev. B* **2005**, *71*, 174436-1−174436-11.

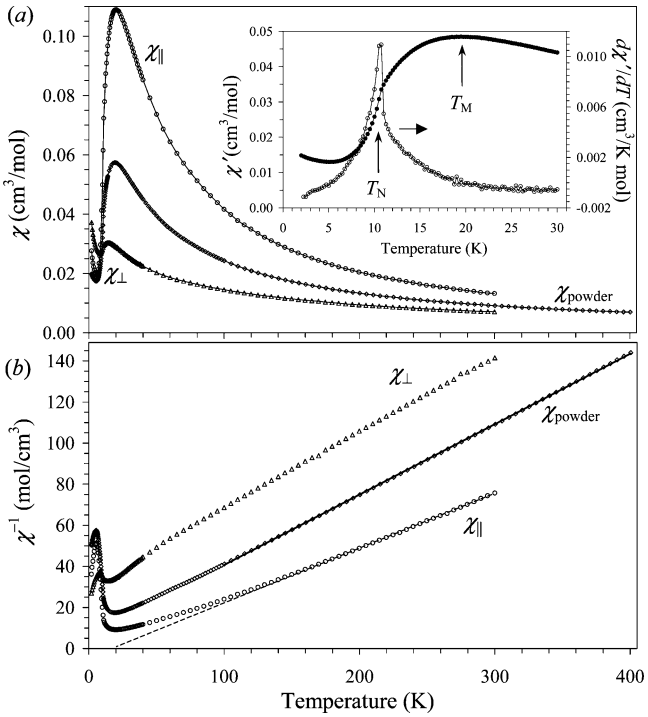

Figure 4. (a) The $\chi(T)$, $\chi_{\parallel}(T)$, and $\chi_{\perp}(T)$ curves (symbols with lines) and (b) the $\chi^{-1}(T)$, $\chi_{\parallel}^{-1}(T)$, and $\chi_{\perp}^{-1}(T)$ curves (symbols) for the powder and aligned $BaCoP_2O_7$ samples measured in FC mode at 100 Oe. The fit to eq 6 is given for the $\chi^{-1}(T)$ curve by the solid line. Inset in panel a gives the $\chi'(T)$ and $d\chi'/dT$ vs T curves for the powder $BaCoP_2O_7$ sample measured by cooling at $H_{ac} = 1$ Oe, $H_{dc} = 0$ Oe, and $f = 10^4$ Hz.

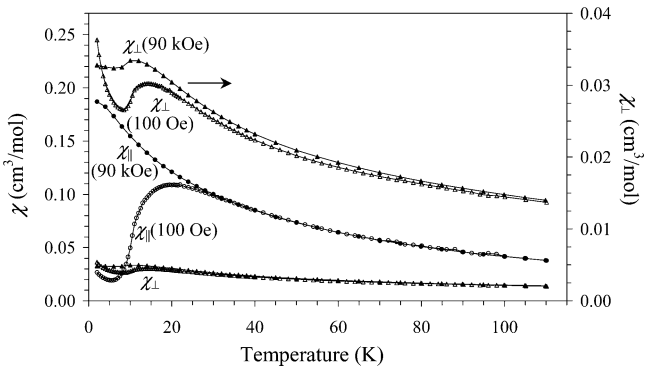

Figure 5. The $\chi_{\parallel}(T)$ and $\chi_{\perp}(T)$ curves (symbols with lines) for the aligned $BaCoP_2O_7$ sample measured in FC mode at 0.1 and 90 kOe. The $\chi_{\perp}(T)$ curves are also plotted using the secondary y axis.

and $BaNiP_2O_7$ have the very close Weiss constants. The negative Weiss constant implies antiferromagnetic interactions between M^{2+} (M = Co and Ni) ions. The effective magnetic moment ($\mu_{eff} = (8C)^{1/2}$) was calculated to be $4.831(2)\mu_B$ per Co^{2+} ion and $3.422(1)\mu_B$ per Ni^{2+} ion. These values are typical for these ions.

The $\chi(T)$ curves showed a broad maximum at $T_M \approx 20.0$ K for $BaCoP_2O_7$ and $T_M \approx 19.0$ K for $BaNiP_2O_7$. The $d(\chi T)/dT$ versus T curves exhibited sharp peaks at $T_N = 10.4$ K for $BaCoP_2O_7$ and $T_N = 10.1$ K for $BaNiP_2O_7$. The forms of the $\chi(T)$ curves indicate the antiferromagnetic ordering at T_N. The large difference between T_N and T_M suggests the presence of a large contribution from the short-range correlations.[19]

The $\chi'(T)$ curves for $BaCoP_2O_7$ were measured between 2 and 30 K and found to be independent of H_{ac}, frequency,

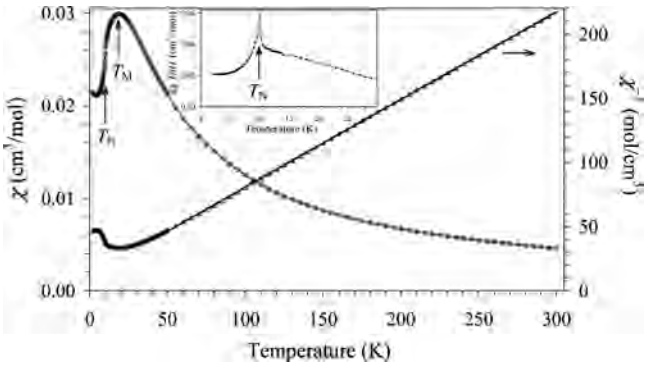

Figure 6. The $\chi(T)$ (circles with lines) and $\chi^{-1}(T)$ (triangles) curves for the powder $BaNiP_2O_7$ sample measured in ZFC mode at 100 Oe. The fit to eq 6 is given for the $\chi^{-1}(T)$ curve by the solid line. Inset shows the $d(\chi T)/dT$ vs T curve between 2 and 30 K.

and heating/cooling mode. The $\chi'(T)$ curves (see the inset of Figure 4) were very close to the $\chi(T)$ curve measured at 100 Oe. No peaks were found on the $\chi'(T)$ curves at T_N. This fact is attributed to the presence of short-range correlations. No anomaly was observed on the $\chi''(T)$ curves. However, the $d\chi'/dT$ versus T curves exhibited sharp peaks at 10.5 K, like those in the $d\chi/dT$ versus T and $d(\chi T)/dT$ versus T curves.

For the aligned $BaCoP_2O_7$ sample, a large difference was observed between the $\chi_{\parallel}(T)$ (magnetic field is parallel to the alignment or easy direction) and $\chi_{\perp}(T)$ (magnetic field is perpendicular to the alignment direction) curves. Such behavior is obviously different from the behavior of a conventional isotropic 3D antiferromagnet. For an isotropic 3D antiferromagnet, the $\chi_{\parallel}(T)$ and $\chi_{\perp}(T)$ curves should coincide above T_N (T_M).[19] The large difference between the $\chi_{\parallel}(T)$ and $\chi_{\perp}(T)$ curves of $BaCoP_2O_7$ may be attributed to a large single-ion anisotropy of Co^{2+} and to the one-dimensional nature of $BaCoP_2O_7$. For example, in $BaCo_2V_2O_8$ with a one-dimensional arrangement of Co^{2+} ions, a large difference was also observed in magnetic susceptibility curves measured along different crystallographic directions.[29]

In the case of $BaCoP_2O_7$, the position of the broad maximum was different for the $\chi_{\parallel}(T)$ and $\chi_{\perp}(T)$ curves at 100 Oe (Figure 5), whereas the peak positions on the $d(\chi_{\parallel}T)/dT$ versus T and $d(\chi_{\perp}T)/dT$ versus T curves, which define T_N, were the same. The $\chi_{\parallel}(T)$ curve for $BaCoP_2O_7$ measured at 90 kOe showed no maximum, however the $\chi_{\perp}(T)$ curve exhibited a small maximum at $T_M \approx 10$ K. The difference between the $\chi_{\parallel}(T)$ curves at 0.1 and 90 kOe suggests the presence of field-induced phase transitions at low-temperatures. Note that specific heat data for $BaCoP_2O_7$ at 90 kOe showed a peak at 9.6 K (see Supporting Information).

Specific heat data for $BaCoP_2O_7$ and $BaNiP_2O_7$ at zero magnetic field showed λ-type anomalies at T_N, confirming the long-range antiferromagntic ordering (Figure 7). The magnetic specific heat, C_m, was calculated as $C_p - C_{lattice}$, where $C_{lattice}$ is the total specific heat of $BaZnP_2O_7$. The large percentage of magnetic entropy, $S_m = \int((C_m)/T)dT$, was gained above T_N (~71 and ~78% of the experimental saturated values for $BaCoP_2O_7$ and $BaNiP_2O_7$, respectively) confirming the large contribution of the short-range correla-

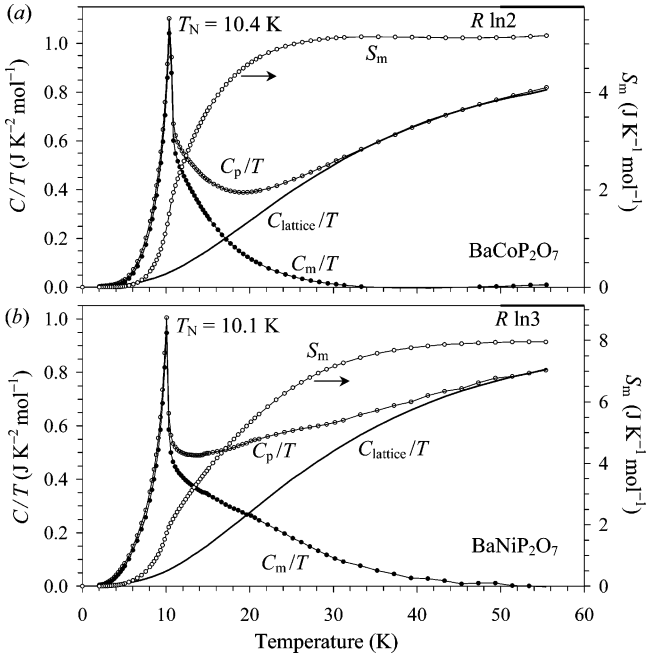

Figure 7. Total specific heat divided by temperature, C_p/T, magnetic specific heat divided by temperature, C_m/T, and magnetic entropy, S_m, plotted against T for (a) $BaCoP_2O_7$ and (b) $BaNiP_2O_7$. Thin solid lines between experimental points are drawn for the eye.

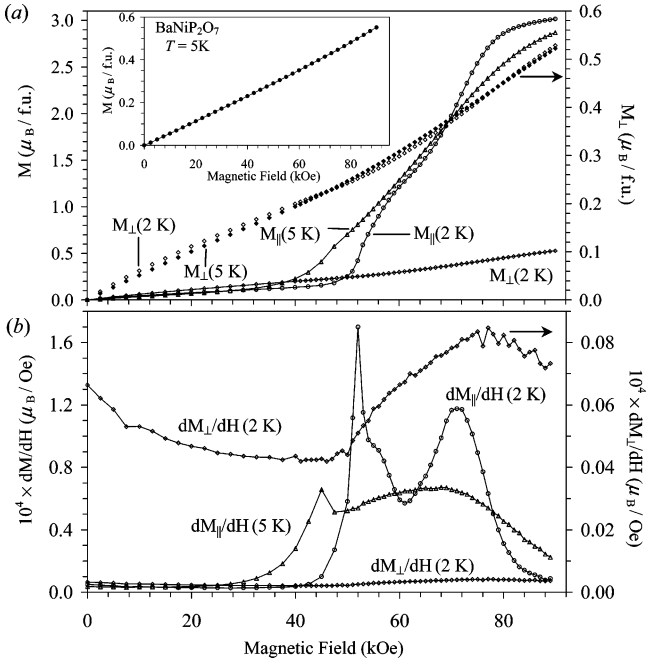

Figure 8. (a) Magnetization curves, $M_\parallel$ vs H and $M_\perp$ vs H, at 2 and 5 K for the aligned $BaCoP_2O_7$ sample. The curves measured from 0 to 90 kOe are shown by symbols and the curves measured from 90 to 0 kOe are given by lines. The $M_\perp$ vs H curves are also presented using the secondary y axis. Inset shows the magnetization curve for the powder $BaNiP_2O_7$ sample at 5 K. (b) The $dM_\parallel/dH$ vs H and $dM_\perp/dH$ vs H curves (symbols with lines; from 0 to 90 kOe) obtained from those in (a) by numerical calculations.

tions. The experimental S_m values were a little bit smaller than the theoretical values of $R \ln(2S + 1)$ with $S = 1/2$ for Co^{2+} and $S = 1$ for Ni^{2+}. Note that at low temperatures, the Co^{2+} ion behaves as an $S = 1/2$ ion.[19]

The magnetization curve, M versus H, at 5 K for the powdered $BaNiP_2O_7$ sample exhibited almost linear behavior and no anomaly up to 90 kOe anticipated for the antiferromagnetic state (inset of Figure 8a). In the case of $BaCoP_2O_7$, the linear behavior was observed up to about 30 kOe (at 5 K) and 50 kOe (at 2 K). Above these fields, we have observed metamagnetic phase transitions on the $M_\parallel$ versus H curves. The $M_\perp$ versus H curves at 2 and 5 K showed small curvatures near 50 kOe, probably because the alignment or the sample position was not perfect. However, these curvatures may also have the intrinsic nature for $BaCoP_2O_7$. The $M_\parallel$ versus H curve at 2 K was saturated at about 3 μ_B/mol expected for the Co^{2+} ion with three unpaired electrons.[19] No hysteresis loop was detected on the $M_\parallel$ versus H and $M_\perp$ versus H curves.

The $dM_\parallel/dH$ versus H curve at 2 K exhibited one sharp peak at 52 kOe and two broad peaks at 55 and 71 kOe (Figure 8b). To investigate the magnetism of $BaCoP_2O_7$ in more detail, we measured the field dependence of the ac susceptibility at 2 and 5 K (Figure 9) and the temperature dependence of the ac susceptibility at a static field of 90 kOe (see Supporting Information). Two peaks at 53 and 74 kOe were clearly observed on the $\chi_\parallel''(H)$ curves at 2 K indicating the appearance of a net ferromagnetic moment. The $\chi_\parallel'(H)$ curves at 2 K showed two rather broad peaks at 56 and 71 kOe. One can see that the $dM_\parallel/dH$ versus H curve is, quantitatively, a sum of the $\chi_\parallel'(H)$ and $\chi_\parallel''(H)$ curves. The $\chi_\parallel'(T)$ curves at $H_{dc} = 90$ kOe were almost frequency independent and exhibited very broad maxima near 10 K,

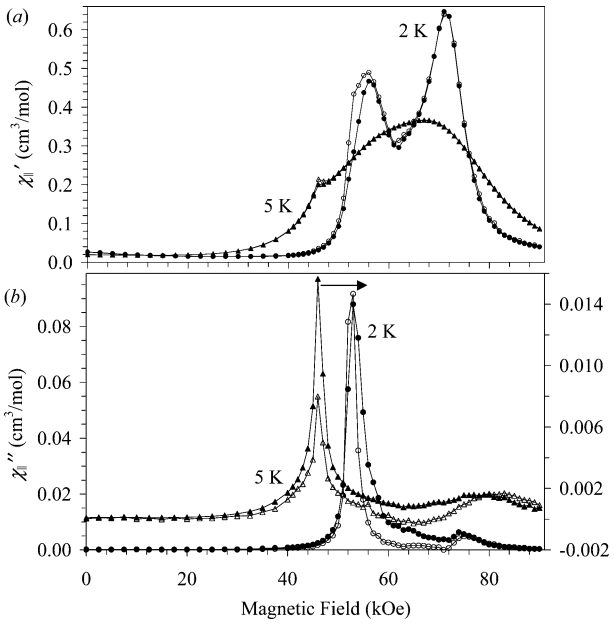

Figure 9. (a) $\chi_\parallel'$ (H, T_{const}) and (b) $\chi_\parallel''$ (H, T_{const}) curves for the aligned $BaCoP_2O_7$ sample measured at 2 K (circles) and 5 K (triangles) with $H_{ac} = 10$ Oe and $f = 10^2$ (empty symbols) and 10^3 Hz (black symbols).

whereas the $\chi_\parallel''(T)$ curves showed maxima near 8 K and strong dependence on the frequency.

The appearance of a small magnetization plateau with a value of about one-half of the saturated value (Figure 8a) suggests the existence of an intermediate ferrimagnetic phase between the antiferromangetic ground state and the ferromagnetic state. It seems that the interaction between Co ions along the easy axis (the alignment direction) is ferromagnetic.

This ferromagnetic moment is compensated by the neighboring units resulting in the antiferromagnetic state. The application of a magnetic field along the easy axis breaks the antiferromagnetic state. The ferromagnetic interaction in $BaCoP_2O_7$ is also shown by a positive Weiss constant of the $\chi_{II}(T)$ curve if it is extrapolated from high-temperature region (Figure 4b). The information about the magnetic structure is required to understand the nature and details of the two metamagnetic phase transitions in $BaCoP_2O_7$. Note that two metamagnetic phase transitions with an intermediate ferrimagnetic state were found in one-dimensional $RbFeCl_3 \cdot 2D_2O$ and $CsFeCl_3 \cdot 2D_2O$.[19,30]

The magnetic behavior of $BaMP_2O_7$ (M = Co, Ni, and Cu) is quite different. Different magnetic behaviors were also found in $CuWO_4$, $CoWO_4$, and $NiWO_4$, despite their close crystal structures.[31] $CuWO_4$ showed a 1D antiferromagnetic short-range order (with $J/k_B = 132.6$ K) above $T_N = 24$ K. $CoWO_4$ and $NiWO_4$ were shown to be ordinary 3D antiferromagnets with $T_N = 48$ and 62 K, respectively, without noticeable short-range correlations in comparison to those of $BaCoP_2O_7$ and $BaNiP_2O_7$.

The interaction between the Cu atoms in $BaCuP_2O_7$, mediated by two super-superexchange paths, is rather strong. Because the magnetic orbitals of Cu^{2+} are strongly anisotropic in shape, the other interactions are very weak and T_N is very low. Another reason for the pronounced 1D nature of $BaCuP_2O_7$ is the quantum effects for a small spin Cu^{2+} ion ($S = 1/2$) in comparison with those of Ni^{2+} and Co^{2+} ions. The large contribution of the short-range (1D) correlations in $BaCoP_2O_7$ and $BaNiP_2O_7$ is confirmed by the specific heat data and the noticeable difference between T_N and T_M. These short-range correlations are consistent with the 1D nature of the isostructural $BaCuP_2O_7$. However, in comparison with $BaCuP_2O_7$, J_1 and J_2 may not be negligible in $BaCoP_2O_7$ and $BaNiP_2O_7$. As far as we are aware, the double-spin chain system (Figure 1a) was investigated extensively only for $S = 1/2$.[1,4,5,32] Therefore, $BaCoP_2O_7$ and $BaNiP_2O_7$ may be good candidate model compounds for the double-spin chain system with $S = 3/2$ and 1. Note that $BaCuP_2O_7$ is a good illustration of the importance of super-superexchange interactions in determining the patterns of strongly interacting exchange paths.[21]

In conclusion, we investigated the magnetic properties of three isostructural compounds $BaCuP_2O_7$, $BaCoP_2O_7$, and $BaNiP_2O_7$. $BaCuP_2O_7$ was shown to be an excellent 1D linear-chain Heisenberg antiferromagnet with $J/k_B = 103.8$ K and $k_BT_N/J = 0.78\%$. $BaCoP_2O_7$ and $BaNiP_2O_7$ are ordered antiferromagnetically at $T_N = 10.4$ and 10.1 K, respectively, and show a large contribution from short-range correlations. $BaCoP_2O_7$ exhibits two metamagnetic phase transitions and 1/2 magnetization plateau.

Acknowledgment. The authors express their thanks to the Ministry of Education, Culture, Sports, Science and Technology, Japan, for Grant-in-Aid No. 12CE2005, for COE Research on Elements Science No. 14204070, and for 21COE on the Kyoto Alliance for Chemistry. ICYS is supported by Special Coordination Funds for Promoting Science and Technology from MEXT, Japan.

Supporting Information Available: Experimental, calculated, and difference XRD patterns for the powder and aligned $BaMP_2O_7$ (M = Co and Cu) samples (Figures S1−S2), C_p/T versus T curves for $BaCoP_2O_7$ at 0, 50, and 90 kOe (Figure S3), DTA curves for $BaMP_2O_7$ (M = Co, Ni, and Cu) (Figure S4), and $\chi_{II}'(T)$ and $\chi_{II}''(T)$ curves of $BaCoP_2O_7$ measured at $H_{dc} = 90$ kOe from 30 to 3 K with $H_{ac} = 10$ Oe and $f = 10^2$, 10^3, 5×10^3, and 10^4 Hz (Figure S5) (PDF). This material is available free of charge via the Internet at http://pubs.acs.org.

IC050938Z

(29) He, Z.; Fu, D.; Kyomen, T.; Taniyama, T.; Itoh, M. *Chem. Mater.* **2005**, *17*, 2924.
(30) Basten, J. A. J.; van Vlimmeren, Q. A. G.; de Jonge, W. J. M. *Phys. Rev. B* **1978**, *5*, 2179−2184.
(31) Yamaguchi, M.; Furuta, T.; Ishikawa, M. *J. Phys. Soc. Jpn.* **1996**, *65*, 2998−3006.
(32) Hase, M.; Kuroe, H.; Ozawa, K.; Suzuki, O.; Kitazawa, H.; Kido, G.; Sekine, T. *Phys. Rev. B* **2004**, *70*, 104426-1−104426-5.